KO of 5-InsP$_7$ kinase activity transforms the HCT116 colon cancer cell line into a hypermetabolic, growth-inhibited phenotype

Chunfang Gu[a], Hoai-Nghia Nguyen[a], Douglas Ganini[b], Zhaowei Chen[c], Henning J. Jessen[d], Zhen Gu[c], Huanchen Wang[a], and Stephen B. Shears[a,1]

[a]Signal Transduction Laboratory, National Institute of Environmental Health Sciences, National Institutes of Health, Research Triangle Park, NC 27709; [b]Immunity, Inflammation and Disease Laboratory, National Institute of Environmental Health Sciences, National Institutes of Health, Research Triangle Park, NC 27709; [c]Joint Department of Biomedical Engineering, University of North Carolina at Chapel Hill and North Carolina State University, Raleigh, NC 27695; and [d]Institute of Organic Chemistry, Albert Ludwigs University, Freiburg, 79104 Freiburg, Germany

Edited by John Blenis, Weill Cornell Medical College, New York, NY, and accepted by Editorial Board Member Gregg L. Semenza September 25, 2017 (received for review February 10, 2017)

The inositol pyrophosphates 5-InsP$_7$ (diphosphoinositol pentakisphosphate) and 1,5-InsP$_8$ (bis-diphosphoinositol tetrakisphosphate) are highly energetic cellular signals interconverted by the diphosphoinositol pentakisphosphate kinases (PPIP5Ks). Here, we used CRISPR to KO PPIP5Ks in the HCT116 colon cancer cell line. This procedure eliminates 1,5-InsP$_8$ and raises 5-InsP$_7$ levels threefold. Expression of p53 and p21 was up-regulated; proliferation and G1/S cell-cycle transition slowed. Thus, PPIP5Ks are potential targets for tumor therapy. Deletion of the PPIP5Ks elevated [ATP] by 35%; both [ATP] and [5-InsP$_7$] were restored to WT levels by overexpression of PPIP5K1, and a kinase-compromised PPIP5K1 mutant had no effect. This covariance of [ATP] with [5-InsP$_7$] provides direct support for an energy-sensing attribute (i.e., 1 mM K_m for ATP) of the 5-InsP$_7$–generating inositol hexakisphosphate kinases (IP6Ks). We consolidate this conclusion by showing that 5-InsP$_7$ levels are elevated on direct delivery of ATP into HCT116 cells using liposomes. Elevated [ATP] in *PPIP5K*$^{-/-}$ HCT116 cells is underpinned by increased mitochondrial oxidative phosphorylation and enhanced glycolysis. To distinguish between 1,5-InsP$_8$ and 5-InsP$_7$ as drivers of the hypermetabolic and p53-elevated phenotypes, we used *IP6K2* RNAi and the pan-IP6K inhibitor, *N*2-(*m*-trifluorobenzyl), *N*6-(*p*-nitrobenzyl) purine (TNP), to return 5-InsP$_7$ levels in *PPIP5K*$^{-/-}$ cells to those of WT cells without rescuing 1,5-InsP$_8$ levels. Attenuation of IP6K restored p53 expression but did not affect the hypermetabolic phenotype. Thus, we conclude that 5-InsP$_7$ regulates p53 expression, whereas 1,5-InsP$_8$ regulates ATP levels. These findings attribute hitherto unsuspected functionality for 1,5-InsP$_8$ to bioenergetic homeostasis.

bioenergetics | signaling | inositol pyrophosphates

Inositol pyrophosphates (PP-InsPs) are diffusible, intracellular signaling molecules with a uniquely crowded arrangement of phosphate and "high-energy" diphosphate groups; up to seven or eight phosphates are tightly distributed around the six-carbon inositol ring, yielding InsP$_7$ and InsP$_8$, respectively (1–3). The highly electronegative and energetic properties of the PP-InsPs enable them to regulate protein function through electrostatic interactions (2) and by protein pyrophosphorylation (4, 5). A number of biological effects have been attributed to the PP-InsPs, but evidence is emerging that a primary role is to regulate metabolic circuitry (1, 2, 6–8) as part of an overarching process by which signaling cascades interface with cellular and organismal homeostasis (9).

Most previous work on the roles of PP-InsPs in metabolic homeostasis has focused on the inositol hexakisphosphate kinases (IP6Ks) that synthesize 5-InsP$_7$ from InsP$_6$ (Fig. 1*A*). Such experiments have, for example, shown that IP6Ks regulate insulin secretion from pancreatic β-cells (10). IP6K1 KO mice exhibit increased adipose tissue browning, insulin sensitivity, and resistance to diet-induced obesity (11, 12). Another metabolic consequence of IP6K KO is an increase in glycolysis and a reduction in mitochondrial oxidative phosphorylation (6). Pharmacological inhibition of IP6K activity in mice enhances thermogenesis and inhibits progression of diet-induced obesity (13), and it also increases mitochondrial mass and ATP levels in cardiomyocytes (14). Thus, 5-InsP$_7$, the IP6K product, is the PP-InsP that has received the most attention in this field. It is also the predominant PP-InsP to accumulate in mammalian cells (15, 16).

Nevertheless, IP6Ks are essential for the synthesis of not only 5-InsP$_7$ but also, 1,5-InsP$_8$ (Fig. 1*A*). Thus, either or both PP-InsPs could, in theory, contribute to any phenotype that results after manipulating IP6K activity. However, with some exceptions (17, 18), this is a complication that does not receive much attention, despite cellular 1,5-InsP$_8$ turnover having some metabolic properties that suggest that it could be an independent signaling molecule. For example, 1,5-InsP$_8$ levels decrease during bioenergetic stress (19, 20). Conversely, in HCT116 colonic epithelial cells, 1,5-InsP$_8$ levels increase several fold in response to raising extracellular [Pi] from 1 to 6 mM (20). These observations underscore the potential value of developing methods that can help to distinguish the individual biological roles of 1,5-InsP$_8$ from 5-InsP$_7$. This has been a major goal of this study.

Significance

Therapeutic improvements to human health can accrue from understanding the bidirectional relationship between cell signaling and bioenergetic homeostasis. Key players in this communication interface are inositol pyrophosphate cellular signals 5-InsP$_7$ and 1,5-InsP$_8$, which are interconverted by diphosphoinositol pentakisphosphate kinases (PPIP5Ks). Here, an intestinal tumor cell line is used for CRISPR-based KO of PPIP5Ks, which eliminates 1,5-InsP$_8$ and raises 5-InsP$_7$ levels several fold. *PPIP5K*$^{-/-}$ cells exhibit a growth-inhibited phenotype, indicating that PPIP5Ks are potential targets for tumor therapy. *PPIP5K*$^{-/-}$ cells also have elevated levels of ATP because of increased mitochondrial biomass and accelerated rates of glycolysis. This hypermetabolic state is attributed to hitherto unsuspected functions for 1,5-InsP$_8$ in bioenergetic homeostasis, thereby suggesting that PPIP5Ks could offer approaches to treat metabolic diseases.

Author contributions: C.G., H.-N.N., D.G., Z.C., Z.G., H.W., and S.B.S. designed research; C.G., H.-N.N., D.G., Z.C., Z.G., and H.W. performed research; H.J.J. contributed new reagents/analytic tools; C.G., H.-N.N., D.G., H.W., and S.B.S. analyzed data; and C.G., H.W., and S.B.S. wrote the paper.

The authors declare no conflict of interest.

This article is a PNAS Direct Submission. J.B. is a guest editor invited by the Editorial Board.

[1]To whom correspondence should be addressed. Email: shears@niehs.nih.gov.

This article contains supporting information online at www.pnas.org/lookup/suppl/doi:10.1073/pnas.1702370114/-/DCSupplemental.

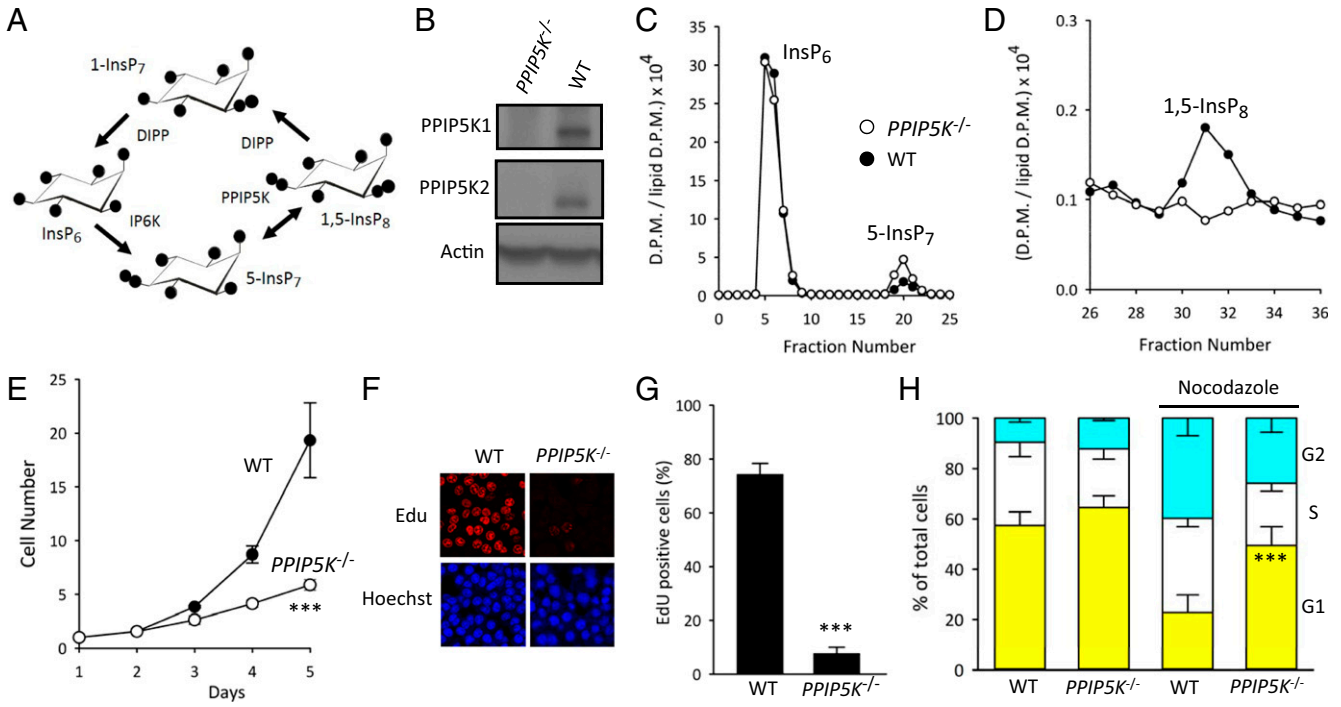

Fig. 1. *PPIP5K*$^{-/-}$ HCT116 cells show reduced cell proliferation. (*A*) A proposed cyclical pathway of PP-InsP turnover involving IP6Ks, PPIP5Ks, and DIPPs (2). *B–H* compare phenotype-relevant parameters obtained from WT and *PPIP5K*$^{-/-}$ HCT116 cells as follows: (*B*) Western analysis of PPIP5K1 and PPIP5K2; (*C* and *D*) HPLC analysis of [^{3}H]InsP$_6$, 5-[^{3}H]InsP$_7$, and [^{3}H]InsP$_8$; (*E*) growth curves; (*F* and *G*) staining with EdU; (*H*) cell-cycle analysis performed either with or without 50 nM nocodazole for 6 h. In *F–H*, data are means ± SEM from three to four independent experiments. ***$P < 0.001$, *PPIP5K*$^{-/-}$ vs. WT. D.P.M., disintegrations per minute.

Diphosphoinositol pentakisphosphate kinases (PPIP5Ks) catalyze the final step in 1,5-InsP$_8$ synthesis (2) (Fig. 1*A*); mammals express two isoforms, PPIP5K1 and PPIP5K2 (21–23). PPIP5Ks are of particular interest, because they maintain 1,5-InsP$_8$ levels through the actions of competing 5-InsP$_7$ kinase and 1,5-InsP$_8$ phosphatase domains (20). The rationale for this study has been that genetic manipulation of PPIP5K catalytic activities is an experimental strategy that can distinguish between the biological functions of 1,5-InsP$_8$ and 5-InsP$_7$. Thus, we used CRISPR to KO both PPIP5Ks in a human cell line, HCT116. This approach leads us to show functionality for PP-InsPs in regulating cell growth and energy metabolism, suggesting that pharmacological targeting of PPIP5Ks offers a potential approach for tumor therapy and for ameliorating metabolic syndromes.

Results and Discussion

***PPIP5K*$^{-/-}$ HCT116 Cells Exhibit Elevated 5-InsP$_7$ Levels and a Growth-Inhibited Phenotype.** We used CRISPR-Cas9 to KO both PPIP5K1 and PPIP5K2 from the colonic epithelial cell line, HCT116, which is a popular human model system for genetic investigations into PP-InsP biology (20, 24, 25). The efficacy of the KO was verified by (*i*) genomic sequencing, (*ii*) Western blot analysis (Fig. 1*B*), (*iii*) the inability of lysates prepared from *PPIP5K*$^{-/-}$ cells to phosphorylate 5-InsP$_7$ to InsP$_8$ (Fig. S1*A*), and (*iv*) the absence of InsP$_8$ in intact *PPIP5K*$^{-/-}$ cells (Fig. 1 *C* and *D*) [PPIP5Ks also have a limited capacity to synthesize 1-InsP$_7$, but that PP-InsP was below detectable levels in both WT HCT116 cells (16) and *PPIP5K*$^{-/-}$ cells (Fig. S1*B*)].

We found that elimination of PPIP5K activity in HCT116 cells is accompanied by a threefold increase in the cellular levels of 5-InsP$_7$, which is nearly 25-fold greater than the quantity of InsP$_8$ that is lost (Fig. 1 *C* and *D*). This is a startling result, which we interrogated by creating another CRISPR-based *PPIP5K*$^{-/-}$ KO, this time using HEK293 cells (Fig. S1*C*). Again, loss of PPIP5K activity is accompanied by a substantial elevation in 5-InsP$_7$ levels (Fig. S1*D*). Interestingly, a similar outcome has previously been reported on deletion of the single PPIP5K ortholog in two microorganisms: *Saccharomyces cerevisiae* and *Cryptococcus neoformans* (26–28); no explanation has previously been offered that might address this result. Our data show this to be a widely conserved phenomenon, and therefore, it is likely to be highly significant.

We found that the increased 5-InsP$_7$ accumulation in *PPIP5K*$^{-/-}$ cells is not driven by a greater supply of InsP$_6$ substrate (Fig. 1*C*) or by higher levels of expression of IP6K2 (Fig. S1*E*). The expression of other *IP6K* genes is not up-regulated, because total IP6K activity in cell lysates was not increased by the PPIP5K KO (Fig. S1*E*). We considered the possibility that loss of InsP$_8$ from *PPIP5K*$^{-/-}$ cells could lead to an activation of IP6K if the latter kinase was normally directly inhibited by InsP$_8$. However, IP6K activity against 20 μM InsP$_6$ is not affected by 1 μM 1,5-InsP$_8$ (Fig. S1*F*), a concentration that is 10-fold higher than that in HCT116 cells (16). However, from data described below, we provide evidence for a physiologic signaling mechanism that is not evident in assays of cell lysates, which nevertheless, enhances IP6K activity in intact *PPIP5K*$^{-/-}$ cells.

A strong phenotype of *PPIP5K*$^{-/-}$ HCT116 cells is a considerable reduction in their proliferation rate (Fig. 1*E*). This is accompanied by a dramatic reduction in 5-ethynyl-2′-deoxyuridine (EdU) labeling of newly synthesized DNA (Fig. 1 *F* and *G*). Cell-cycle analysis indicated a slowed G1/S-phase transition that was particularly pronounced after nocodazole treatment (Fig. 1*H*). There was no change in the generation of reactive oxygen species or pRb expression or the expression of two proinflammatory cytokines, IL-8 and IFN-β (Fig. S2). Thus, according to current criteria (29), inhibition of proliferation in *PPIP5K*$^{-/-}$ HCT116 cells does not seem to reflect acquisition of a senescent state. PPIP5K knockdown in HEK293 cells also decreased proliferation rate (Fig. S3*A*), which was associated with a slower G1 to S transition after nocodazole treatment (Fig. S3*B*), although these effects were not as strong as in HCT116 cells (Fig. 1 *E* and *H*).

5-InsP$_7$ Regulates p53 Expression. A major goal of this study has been to establish an experimental paradigm for intact cells that can distinguish the functions of 5-InsP$_7$ from those of 1,5-InsP$_8$. We noted that previous work (24) showed 5-InsP$_7$ to stimulate the Tti1/Tti2/Tel2/DNA-PK/ATM cascade, which up-regulates expression of the p53 protein (30). We observed that the higher levels of 5-InsP$_7$ in our *PPIP5K*$^{-/-}$ HCT116 cells (Fig. 1*C*) are associated with up-regulated expression of p53 (Fig. 2*A*). Expression of p21, a cell-cycle inhibitor, is also elevated in *PPIP5K*$^{-/-}$ HCT116 cells (Fig. S4), which may contribute to the slowed cell-cycle transition (Fig. 1*H*). Expression of both p53 and p21 is also elevated in *PPIP5K*$^{-/-}$ HEK293 cells (Fig. S1*C*).

In *PPIP5K*$^{-/-}$ HCT116 cells, levels of p53 expression and cellular [5-InsP$_7$] and [1,5-InsP$_8$] were all restored to WT levels on transfection of PPIP5K1 (Fig. 2 *B*–*D* and Fig. S5). The PPIP5K1^{D332A} kinase-impaired mutant had no effect (Fig. 2 *B* and *C*). Since PPIP5Ks contain separate 1-kinase and 1-phosphatase domains (20), we transfected *PPIP5K*$^{-/-}$ cells with the "hyperkinase" PPIP5K1^{R399A} phosphatase mutant (Fig. S5). This approach rescued levels of p53 and 5-InsP$_7$; the 1,5-InsP$_8$ levels now surpassed those of WT cells (Fig. 2 *B*–*D*). These data indicate that p53 expression is normally repressed by PPIP5K catalytic activity. While 1-InsP$_7$ is potentially functional, it did not reach detectable levels, even after expression of the hyperkinase PPIP5K1^{R399A} phosphatase mutant (Fig. S1*B*). Thus, we propose that, in *PPIP5K*$^{-/-}$ cells, p53 expression is either stimulated by the increased [5-InsP$_7$] or inhibited by loss of 1,5-InsP$_8$. To distinguish between these two alternatives, we treated *PPIP5K*$^{-/-}$ cells with a submaximally effective concentration of *N*2-(*m*-trifluorobenzyl), *N*6-(*p*-nitrobenzyl) purine (TNP), a pan-IP6K inhibitor (26), specifically to return 5-InsP$_7$ levels to those of WT cells (Fig. 2 *E*–*G*); this procedure does not rescue 1,5-InsP$_8$ levels (Fig. 1*A*). In contrast, this TNP treatment returned p53 expression to the level seen in WT cells (Fig. 2*H*). Thus, we conclude that 5-InsP$_7$ stimulates p53 expression, consistent with previous work (24, 30). These experiments serve as proof of principle that, in *PPIP5K*$^{-/-}$ cells, separate functions of 5-InsP$_7$ and 1,5-InsP$_8$ can be resolved by attenuation of IP6K.

Loss of InsP$_8$ from *PPIP5K*$^{-/-}$ Cells Promotes a Hypermetabolic Phenotype. Most of the work on the roles of PP-InsPs in bioenergetic homoeostasis has focused on the IP6Ks that synthesize 5-InsP$_7$ from InsP$_6$. For example, cellular levels of ATP have been shown to be elevated on KO of IP6K activity in MEFs (mouse embryonic fibroblasts) (6) and after TNP-mediated inhibition of IP6K in cardiomyocytes (14). We note here that both experimental approaches would have reduced levels of 1,5-InsP$_8$ as well as 5-InsP$_7$. This is a significant point, because we found that ATP levels are higher in both *PPIP5K*$^{-/-}$ HCT116 cells and *PPIP5K*$^{-/-}$ HEK293 cells compared with the corresponding WT cells (Fig. 3*A*). However, in both cell types, PPIP5K KO is associated with increased levels of 5-InsP$_7$ (Fig. 1*C* and Fig. S1*D*). Thus, in four different mammalian cell lines—MEFs (6), cardiomyocytes (14), HCT116 cells (Fig. 3*A*), and HEK293 cells (Fig. 3*A*)—the change in PP-InsP turnover that is consistently associated with elevated [ATP] is a loss of 1,5-InsP$_8$ rather than an effect on 5-InsP$_7$ levels.

The elevation in ATP levels in *PPIP5K*$^{-/-}$ cells was significantly reversed by transfection of either WT PPIP5K1 or the PPIP5K1^{R399A} phosphatase mutant but not by the PPIP5K1^{D332A} kinase mutant (Fig. 3*B*), thereby underscoring that changes in 5-InsP$_7$ kinase activity are what underlies the hypermetabolic phenotype of *PPIP5K*$^{-/-}$ cells. To further pursue which PP-InsP is responsible, we used TNP to reduce IP6K activity in *PPIP5K*$^{-/-}$ cells (as described above). This did not affect ATP levels (Fig. 3*C*). We

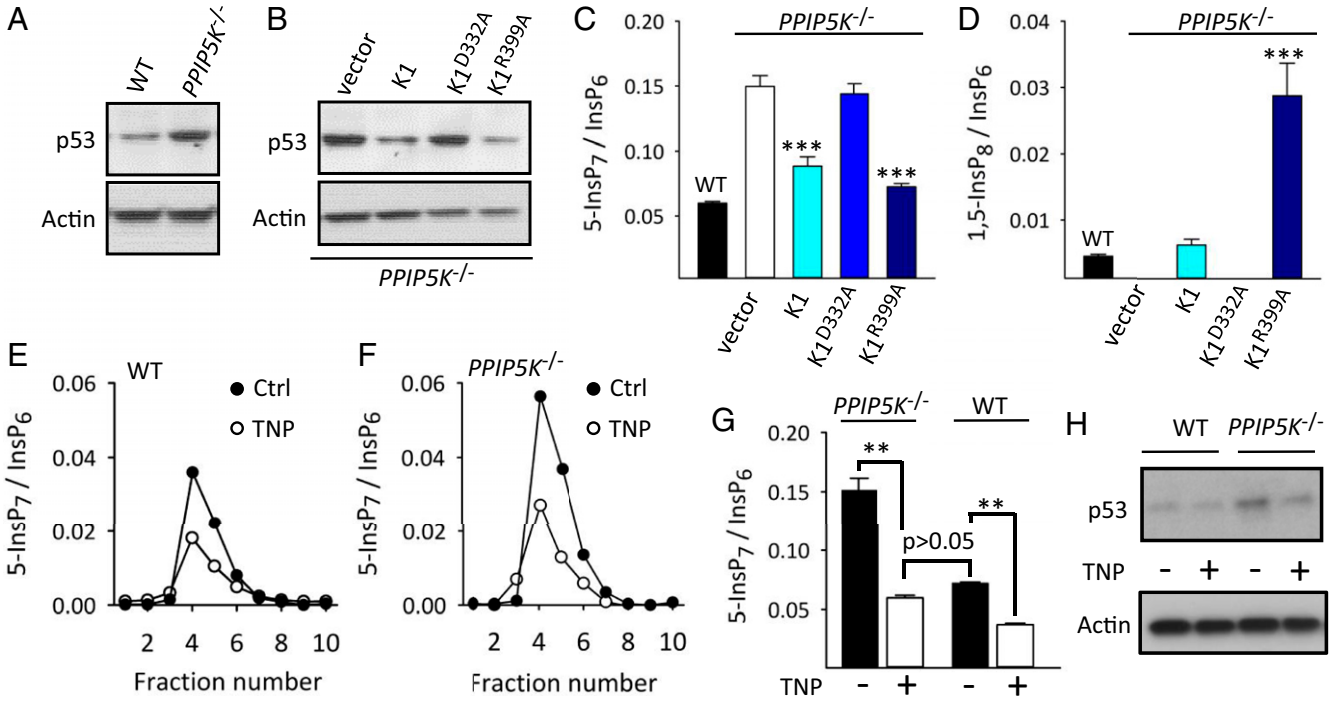

Fig. 2. The influence of PP-InsP turnover on p53 expression. HCT116 cells used in these experiments were, as indicated, WT, *PPIP5K*$^{-/-}$, or *PPIP5K*$^{-/-}$ transfected with vector, PPIP5K1 (K1), the D332A kinase mutant, or the R399A phosphatase mutant. (*A* and *B*) Representative Western analyses of p53 expression. (*C* and *D*) Levels of 5-InsP$_7$ and 1,5-InsP$_8$, respectively, determined by HPLC. Bar graphs display means ± SEM from three independent experiments. ***$P < 0.001$ vs. cells transfected with vector alone. (*E* and *F*) Representative HPLC analyses of 5-InsP$_7$ levels in extracts prepared from WT and *PPIP5K*$^{-/-}$ cells, respectively, after 48 h of treatment with either 10 μM TNP (white circles) or vehicle (Ctrl; black circles). (*G*) Bar graphs show means ± SEM from five experiments as described by *E* and *F*. **$P < 0.01$ (one-way ANOVA). (*H*) Western analysis of p53 expression in WT and *PPIP5K*$^{-/-}$ cells after 48 h of treatment with either 10 μM TNP or vehicle.

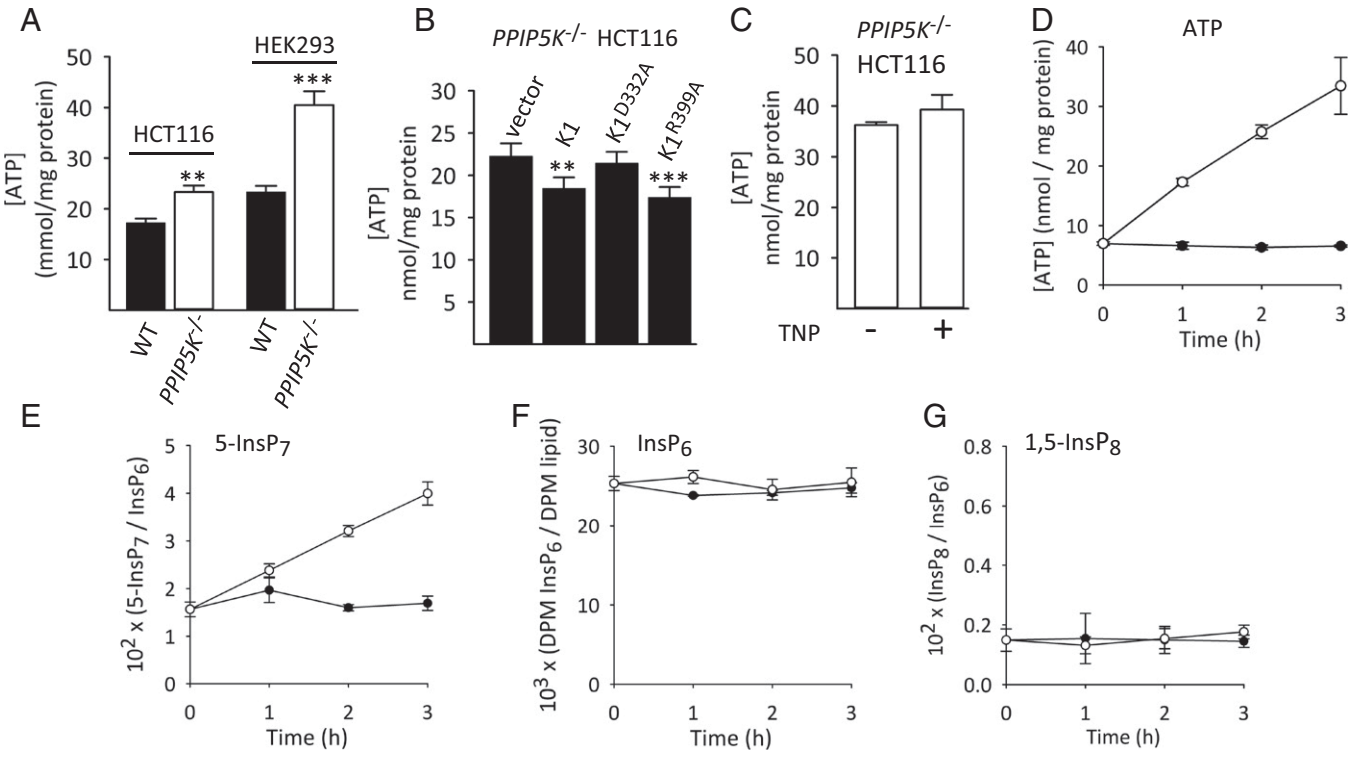

Fig. 3. 1,5-$InsP_8$ levels and cellular [ATP] are interrelated. (*A*) ATP levels in WT (black bars) and *PPIP5K*$^{-/-}$ (white bars) HCT116 and HEK293 cells, respectively. Data are means ± SEM from seven independent experiments. $^{**}P < 0.02$ vs. corresponding WT cells; $^{***}P < 0.001$ vs. corresponding WT cells. (*B*) Levels of ATP in *PPIP5K*$^{-/-}$ HCT116 cells transfected with vector, PPIP5K1 (K1), the D332A kinase mutant, or the R399A phosphatase mutant. Data are means ± SEM from eight independent experiments. $^{**}P < 0.02$ vs. vector control; $^{***}P < 0.01$ vs. vector control. (*C*) ATP levels in *PPIP5K*$^{-/-}$ HCT116 cells incubated for 48 h with either vehicle or 10 μM TNP. Data are means ± SEM from seven independent experiments. (*D–G*) [ATP], [5-$InsP_7$], [$InsP_6$], and [$InsP_8$], respectively, in WT HCT116 cells incubated in glucose-free medium for 18 h before addition of either ATP-loaded liposomes (open circles) or empty liposomes (closed circles) for the indicated times. Data are means ± SEM from three independent experiments.

also reduced 5-$InsP_7$ levels in *PPIP5K*$^{-/-}$ cells by RNAi against *IP6K2* (Fig. S6*A*), the major source of 5-$InsP_7$ in HCT116 cells (Fig. S6*B*) (25); again, [ATP] was not affected (Fig. S6*C*). Thus, we conclude that, in *PPIP5K*$^{-/-}$ cells, elevated [ATP] is because of the loss of 1,5-$InsP_8$, not the gain of 5-$InsP_7$. Additionally, [ATP] was not affected on inhibition of p53 with pifithrin-α (Fig. S6*D*). This negative result is significant, because expression of p53, a master metabolic regulator (31), is up-regulated downstream of 5-$InsP_7$ (see above).

Our conclusion that elevated levels of 5-$InsP_7$ in *PPIP5K*$^{-/-}$ cells do not promote the associated increase in [ATP] prompted us to next investigate if, conversely, it might be [ATP] that regulates [5-$InsP_7$]. Indeed, it is a long-standing proposal (32) that 5-$InsP_7$ synthesis is tied to cellular bioenergetic status through the unusually low K_m value for ATP (1 mM) of the IP6Ks. However, direct evidence that this mechanism operates in intact cells has been lacking. Thus, we starved WT HCT116 cells of glucose overnight; this caused ATP levels to fall from 17 (Fig. 3*A*) to 7 nmol/mg protein (zero time point in Fig. 3*D*). In parallel, 5-$InsP_7$ levels dropped from a value of around 0.05 (as a ratio to [$InsP_6$]) (Fig. 2*C*) to 0.015 (zero time point in Fig. 3*E*). Next, we rescued ATP levels directly by using liposomes as a vehicle for delivering the nucleotide directly into cells (33). Cellular levels of both ATP and 5-$InsP_7$ rose in parallel time courses (Fig. 3 *D* and *E*). The degree of the increase in 5-$InsP_7$ levels was also dependent on the concentration of ATP-loaded liposomes that were added to the cells (Fig. S7). The effect on 5-$InsP_7$ is specific; levels of $InsP_6$ and $InsP_8$ did not change (Fig. 3 *F* and *G* and Fig. S7). Thus, our data provide direct support for the idea (32) that IP6K-driven 5-$InsP_7$ synthesis is a specific metabolic sensor response.

We explored how the absence of 1,5-$InsP_8$ might modify metabolic parameters to facilitate [ATP] being increased. We recorded mitochondrial mass in *PPIP5K*$^{-/-}$ HCT116 cells using Mitotracker Green (MTG). Microscopic analysis indicated that mitochondria in *PPIP5K*$^{-/-}$ HCT116 cells are more tubular and less fragmented compared with WT cells (Fig. 4*A*); such a phenomenon is associated with enhanced oxidative phosphorylation (34). Analysis by flow cytometry recorded a 30% increase in median MTG fluorescence intensity in the *PPIP5K*$^{-/-}$ cells (Fig. 4 *B* and *C*), indicating increased mitochondrial mass. We also assessed mitochondrial bioenergetic competence in both WT and *PPIP5K*$^{-/-}$ HCT116 cells by extracellular flux analysis using Seahorse technology. *PPIP5K*$^{-/-}$ cells show the following percentage increases in oxygen consumption under various conditions: basal, 53%; ATP-coupled, 39%; and maximal, 108% (Fig. 4*D* and Fig. S8*A*). These data are consistent with the mitochondrial biomass being increased. Nevertheless, the "spare respiratory capacity" (35) of the mitochondria in *PPIP5K*$^{-/-}$ cells outstripped that of the WT cells by a greater degree (i.e., 5.5-fold) (Fig. S8*A*) than can be accounted for by the increase in mitochondrial biomass alone (Fig. 4*C*). Thus, it can be concluded that the loss of 1,5-$InsP_8$ after PPIP5K KO in HCT116 cells also elevates mitochondrial bioenergetic capacity.

We also recorded higher rates of extracellular acidification by the *PPIP5K*$^{-/-}$ HCT116 cells, indicative of up-regulation of glycolytic lactate production (Fig. 4*E* and Fig. S8*B*). This conclusion was confirmed by direct assays showing elevated glucose consumption and lactate production in *PPIP5K*$^{-/-}$ cells (Fig. 4 *F* and *G*) that could also contribute to elevated [ATP]. Thus, in HCT116 cells, glycolysis and mitochondrial respiration are not

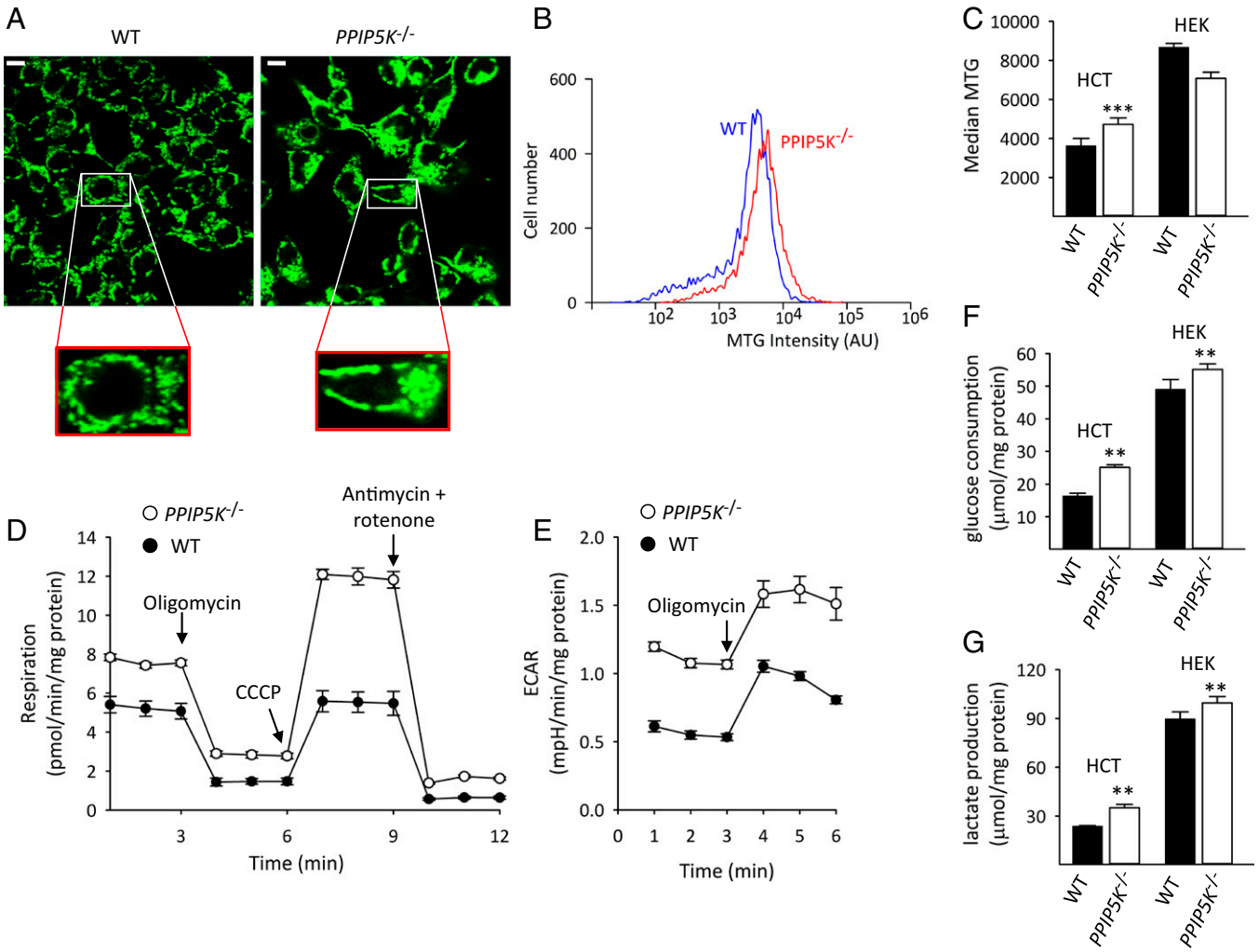

Fig. 4. Bioenergetic metabolism in WT and *PPIP5K*$^{-/-}$ cells. (*A*) Microscopic analysis of WT and *PPIP5K*$^{-/-}$ HCT116 cells labeled with MTG. (Scale bar: 10 µm.) (*B*) Representative analysis of MTG labeling of WT and *PPIP5K*$^{-/-}$ HCT116 cells by flow cytometry. (*C*) Means ± SEM of flow cytometry analysis of MTG labeling of WT (black bars) and *PPIP5K*$^{-/-}$ (white bars) HCT116 cells and HEK293 cells; $n = 7$ for HCT116 cells, and $n = 3$ for HEK293 cells. ***$P < 0.001$. (*D* and *E*) Representative respiration rates and extracellular acidification rates (ECARs), respectively, for WT HCT116 cells (black circles) and *PPIP5K*$^{-/-}$ HCT116 cells (white circles). Data are means ± SEM from five technical replicates. Data combined from four independent experiments are shown in Fig. S8. (*F* and *G*) Glucose consumption and lactate production, respectively, from WT (black bars) and *PPIP5K*$^{-/-}$ (white bars) HCT116 cells and HEK293 cells; means ± SEMs are from four to five independent experiments. **$P < 0.02$ vs. corresponding WT cells.

reciprocally regulated. Such a phenomenon is not entertained by the classical Warburg hypothesis. However, this is not the current viewpoint of cancer cell metabolism. Instead, it is accepted that different tumor populations may utilize varied bioenergetic strategies to satisfy their high-energy requirements (36).

The elevated MTG signal in *PPIP5K*$^{-/-}$ cells is insensitive to either TNP (Fig. S9*A*) or RNAi against *IP6K2* (Fig. S9*B*), indicating that it is not gain of 5-InsP$_7$ but loss of 1,5-InsP$_8$ that promotes elevated mitochondrial biomass. That conclusion is also consistent with previously published data showing increased mitochondrial mass in cardiomyocytes after pharmacological inhibition of IP6K (which inhibits 1,5-InsP$_8$ synthesis) (14). Furthermore, previous work with *IP6K1*$^{-/-}$ adipocytes found a higher rate of uncoupled respiratory activity of mitochondria (13), which could also reflect increased mitochondrial mass.

The elevated rates of glucose consumption and lactate production in *PPIP5K*$^{-/-}$ HCT116 cells were not reversed by either treatment with TNP or by RNAi against *IP6K2* (Fig. S9 *C–F*), indicating that glycolysis is not stimulated by elevated levels of 5-InsP$_7$. Instead, we propose that glycolysis is deinhibited on depletion of 1,5-InsP$_8$ in *PPIP5K*$^{-/-}$ cells. A previous study (6) has described elevated rates of glycolysis in *IP6K1*$^{-/-}$ MEFs (i.e., cells in which levels of both 5-InsP$_7$ and 1,5-InsP$_8$ are reduced). However, glycolysis is unaffected by deletion of *IP6K1* in adipocytes, but mitochondrial respiration is increased (13). As for HEK293 *PPIP5K*$^{-/-}$ cells, they show elevated rates of glycolysis (Fig. 4 *F* and *G*), although mitochondrial mass does not increase (Fig. 4*C*). Nevertheless, in each of these mammalian cell types as well as in HCT116 cells, a hypermetabolic phenotype (i.e., elevated [ATP]) is consistently associated with depletion of 1,5-InsP$_8$.

Concluding Comments

This study breaks ground in its approach to studying metabolic regulation by PP-InsPs. Previous work in this field has focused on proposed functions for 5-InsP$_7$ based on data obtained after genetic and/or pharmacological manipulation of the IP6Ks. Despite 1,5-InsP$_8$ synthesis also being dependent on IP6Ks, that particular PP-InsP has received little attention as a regulator of bioenergetic homeostasis. *PPIP5K*$^{-/-}$ cells have allowed us to show that ATP levels are elevated in the absence of 1,5-InsP$_8$. This result generates a hypothesis that 1,5-InsP$_8$ normally exerts a constraint on ATP synthesis. Consequently, our previous report that 1,5-InsP$_8$

levels fall when cells undergo relatively mild bioenergetic stress (19) may now be viewed as a potential adaptive response that upregulates ATP synthesis. In *PPIP5K*$^{-/-}$ HCT116 cells, increased [ATP] (Fig. 3*A*) reflects greater glycolytic and mitochondrial activities; such expansive metabolic changes likely involve more than one molecular mechanism of action for 1,5-$InsP_8$. Our data also provide direct support for the idea (32) that, in intact cells, IP6K-driven 5-$InsP_7$ synthesis is a sensor of cellular ATP levels. This is a mechanism that is not exposed by assays of IP6K activity in cell-free lysates in which [ATP] is held constant (Fig. S1*E*).

Our data indicate that deinhibition of ATP synthesis on depletion of 1,5-$InsP_8$ is responsible for the elevation of 5-$InsP_7$ levels in *PPIP5K*$^{-/-}$ cells. A substantial increase in 5-$InsP_7$ levels has also been observed on *PPIP5K* KO in two species of microorganisms: *S. cerevisiae* and *C. neoformans* (26–28); thus, functionality of 1,5-$InsP_8$ as an inhibitor of ATP production may be extremely well conserved. It has also been proposed that PP-InsP turnover is cyclical in nature (2) (Fig. 1*A*). Interruption of such cyclical PP-InsP flux, by elimination of PPIP5Ks, could disturb the dynamic metabolic equilibrium between 5-$InsP_7$ and $InsP_8$, accentuating accumulation of 5-$InsP_7$.

Among major targets for the treatment of metabolic diseases, such as diabetes and obesity, is to increase glucose consumption (37). *PPIP5K*$^{-/-}$ cells display just such a phenotype. Thus, pharmacological targeting of PPIP5Ks may have beneficial effects in metabolic diseases. Finally, the finding that the proliferation rate of the HCT116 colonic epithelial cell line is particularly susceptible to PPIP5K knockdown suggests that this enzyme might be a therapeutic target in tumor biology.

Materials and Methods

Cell Culture. HEK293 and HCT116 cells were cultured in DMEM or DMEM/F12, respectively, each supplemented with 10% FBS (Germini Bio-product) and 100 U/mL Penicillin-Streptomycin (ThermoFisher Scientific) at 37 °C with 5% CO_2. Details for CRISPR-based PPIP5K KO and other genetic manipulations are given in *SI Materials and Methods*.

Assays. Assays of enzyme activity and protein levels by Western blotting; assays of cellular [ATP], glucose consumption, and lactate production and metabolic analyses using Seahorse technology; mitochondrial mass analysis using microscopy and flow cytometry; growth curve assays; cell-cycle analysis; and assays of cellular inositol phosphates are described in *SI Materials and Methods*.

Preparation of ATP-Loaded Liposomes. These procedures, which are adapted from ref. 33, are described in *SI Materials and Methods*.

Statistics. Statistical significance was assessed by paired *t* tests or where stated, one-way ANOVA; $P < 0.05$ is considered significant.

ACKNOWLEDGMENTS. D.G. and S.B.S. thank Dr. Ron Mason [National Institute of Environmental Health Sciences (NIEHS)] for his support. Research was supported by the Intramural Research Program of the NIH, NIEHS. H.J.J. received support from Swiss National Science Foundation Grant PP00P2_157607. Z.G. acknowledges a Sloan Research Fellowship from the Alfred P. Sloan Foundation.

1. Azevedo C, Saiardi A (2017) Eukaryotic phosphate homeostasis: The inositol pyrophosphate perspective. *Trends Biochem Sci* 42:219–231.
2. Shears SB (May 19, 2017) Intimate connections: Inositol pyrophosphates at the interface of metabolic regulation and cell signaling. *J Cell Physiol*, 10.1002/jcp.26017.
3. Thota SG, Bhandari R (2015) The emerging roles of inositol pyrophosphates in eukaryotic cell physiology. *J Biosci* 40:593–605.
4. Bhandari R, et al. (2007) Protein pyrophosphorylation by inositol pyrophosphates is a posttranslational event. *Proc Natl Acad Sci USA* 104:15305–15310.
5. Saiardi A, et al. (2004) Phosphorylation of proteins by inositol pyrophosphates. *Science* 306:2101–2105.
6. Szijgyarto Z, Garedew A, Azevedo C, Saiardi A (2011) Influence of inositol pyrophosphates on cellular energy dynamics. *Science* 334:802–805.
7. Wu M, Chong LS, Perlman DH, Resnick AC, Fiedler D (2016) Inositol polyphosphates intersect with signaling and metabolic networks via two distinct mechanisms. *Proc Natl Acad Sci USA* 113:E6757–E6765.
8. Barker CJ, Berggren PO (2013) New horizons in cellular regulation by inositol polyphosphates: Insights from the pancreatic β-cell. *Pharmacol Rev* 65:641–669.
9. Gomes AP, Blenis J (2015) A nexus for cellular homeostasis: The interplay between metabolic and signal transduction pathways. *Curr Opin Biotechnol* 34:110–117.
10. Illies C, et al. (2007) Requirement of inositol pyrophosphates for full exocytotic capacity in pancreatic beta cells. *Science* 318:1299–1302.
11. Chakraborty A, et al. (2010) Inositol pyrophosphates inhibit Akt signaling, thereby regulating insulin sensitivity and weight gain. *Cell* 143:897–910.
12. Zhu Q, Ghoshal S, Tyagi R, Chakraborty A (2016) Global IP6K1 deletion enhances temperature modulated energy expenditure which reduces carbohydrate and fat induced weight gain. *Mol Metab* 6:73–85.
13. Zhu Q, et al. (2016) Adipocyte-specific deletion of Ip6k1 reduces diet-induced obesity by enhancing AMPK-mediated thermogenesis. *J Clin Invest* 126:4273–4288.
14. Sun D, et al. (2015) Oncostatin M (OSM) protects against cardiac ischaemia/reperfusion injury in diabetic mice by regulating apoptosis, mitochondrial biogenesis and insulin sensitivity. *J Cell Mol Med* 19:1296–1307.
15. Lin H, et al. (2009) Structural analysis and detection of biological inositol pyrophosphates reveal that the family of VIP/diphosphoinositol pentakisphosphate kinases are 1/3-kinases. *J Biol Chem* 284:1863–1872.
16. Gu C, Wilson MSC, Jessen HJ, Saiardi A, Shears SB (2016) Inositol pyrophosphate profiling of two HCT116 cell lines uncovers variation in InsP8 levels. *PLoS One* 11: e0165286.
17. Fu C, et al. (2017) Neuronal migration is mediated by inositol hexakisphosphate kinase 1 via α-actinin and focal adhesion kinase. *Proc Natl Acad Sci USA* 114:2036–2041.
18. Pulloor NK, et al. (2014) Human genome-wide RNAi screen identifies an essential role for inositol pyrophosphates in Type-I interferon response. *PLoS Pathog* 10:e1003981, and erratum (2014) 10:e1004519.
19. Choi K, Mollapour E, Choi JH, Shears SB (2008) Cellular energetic status supervises the synthesis of bis-diphosphoinositol tetrakisphosphate independently of AMP-activated protein kinase. *Mol Pharmacol* 74:527–536.
20. Gu C, et al. (2017) The significance of the bifunctional kinase/phosphatase activities of diphosphoinositol pentakisphosphate kinases (PPIP5Ks) for coupling inositol pyrophosphate cell signaling to cellular phosphate homeostasis. *J Biol Chem* 292:4544–4555.
21. Mulugu S, et al. (2007) A conserved family of enzymes that phosphorylate inositol hexakisphosphate. *Science* 316:106–109.
22. Fridy PC, Otto JC, Dollins DE, York JD (2007) Cloning and characterization of two human VIP1-like inositol hexakisphosphate and diphosphoinositol pentakisphosphate kinases. *J Biol Chem* 282:30754–30762.
23. Choi JH, Williams J, Cho J, Falck JR, Shears SB (2007) Purification, sequencing, and molecular identification of a mammalian PP-InsP5 kinase that is activated when cells are exposed to hyperosmotic stress. *J Biol Chem* 282:30763–30775.
24. Rao F, et al. (2014) Inositol pyrophosphates mediate the DNA-PK/ATM-p53 cell death pathway by regulating CK2 phosphorylation of Tti1/Tel2. *Mol Cell* 54:119–132.
25. Koldobskiy MA, et al. (2010) p53-Mediated apoptosis requires inositol hexakisphosphate kinase-2. *Proc Natl Acad Sci USA* 107:20947–20951.
26. Padmanabhan U, Dollins DE, Fridy PC, York JD, Downes CP (2009) Characterization of a selective inhibitor of inositol hexakisphosphate kinases: Use in defining biological roles and metabolic relationships of inositol pyrophosphates. *J Biol Chem* 284:10571–10582.
27. Onnebo SM, Saiardi A (2009) Inositol pyrophosphates modulate hydrogen peroxide signalling. *Biochem J* 423:109–118.
28. Lev S, et al. (2015) Fungal inositol pyrophosphate IP7 is crucial for metabolic adaptation to the host environment and pathogenicity. *MBio* 6:e00531–e15.
29. Sharpless NE, Sherr CJ (2015) Forging a signature of in vivo senescence. *Nat Rev Cancer* 15:397–408.
30. Malbert-Colas L, et al. (2014) HDMX folds the nascent p53 mRNA following activation by the ATM kinase. *Mol Cell* 54:500–511.
31. Berkers CR, Maddocks OD, Cheung EC, Mor I, Vousden KH (2013) Metabolic regulation by p53 family members. *Cell Metab* 18:617–633.
32. Voglmaier SM, et al. (1996) Purified inositol hexakisphosphate kinase is an ATP synthase: Diphosphoinositol pentakisphosphate as a high-energy phosphate donor. *Proc Natl Acad Sci USA* 93:4305–4310.
33. Liang W, Levchenko TS, Torchilin VP (2004) Encapsulation of ATP into liposomes by different methods: Optimization of the procedure. *J Microencapsul* 21:251–261.
34. Wai T, Langer T (2016) Mitochondrial dynamics and metabolic regulation. *Trends Endocrinol Metab* 27:105–117.
35. Brand MD, Nicholls DG (2011) Assessing mitochondrial dysfunction in cells. *Biochem J* 435:297–312.
36. Potter M, Newport E, Morten KJ (2016) The Warburg effect: 80 Years on. *Biochem Soc Trans* 44:1499–1505.
37. Wu C, et al. (2005) Enhancing hepatic glycolysis reduces obesity: Differential effects on lipogenesis depend on site of glycolytic modulation. *Cell Metab* 2:131–140.
38. Ran FA, et al. (2013) Genome engineering using the CRISPR-Cas9 system. *Nat Protoc* 8: 2281–2308.
39. Safrany ST, et al. (1999) The diadenosine hexaphosphate hydrolases from Schizosaccharomyces pombe and Saccharomyces cerevisiae are homologues of the human diphosphoinositol polyphosphate phosphohydrolase. Overlapping substrate specificities in a MutT-type protein. *J Biol Chem* 274:21735–21740.
40. Wang H, DeRose EF, London RE, Shears SB (2014) IP6K structure and the molecular determinants of catalytic specificity in an inositol phosphate kinase family. *Nat Commun* 5:4178.
41. Ganini D, et al. (2017) Fluorescent proteins such as eGFP lead to catalytic oxidative stress in cells. *Redox Biol* 12:462–468.